

HYDROGEOCHEMICAL CHARACTERISTICS OF THE TINTO AND ODIEL RIVERS (SW SPAIN). FACTORS CONTROLLING METAL CONTENTS.

C.R. Cánovas^a, M. Olías^{a,*}, J.M. Nieto^b, A.M. Samiento^b, J.C. Cerón^a

^a Department of Geodynamics and Palaeontology, University of Huelva, Campus 'El Carmen',
21071 Huelva, Spain

^b Department of Geology, University of Huelva, Campus 'El Carmen', 21071 Huelva, Spain

* Corresponding author:

M. Olías

Tel: +34 95 921 9864 Fax: +34 95 921 9440 E-mail: manuel.olias@dgyp.uhu.es

Dpto. Geodinámica y Paleontología, Universidad de Huelva, Campus 'El Carmen', 21071 Huelva, SPAIN.

Abstract

The Tinto and Odiel Rivers are strongly affected by AMD due to the intense sulphur mining developed in their basins since nearly 5000 years. In this study the results obtained from a weekly sampling in both rivers, before their mouth in the Ría of Huelva, over three years and a half of control are analysed. In the Tinto River, sulphates, Al, Cd, Co, Li and Zn concentration doubles the Odiel values. However, Fe concentration in the Odiel River is 20 times lower, since neutralization processes are more intense. Lower As, Cr, Cu and Pb concentrations are also found in the Odiel River as, to a greater or lesser extent, they are sorpted and coprecipitated with Fe. Other elements such as Be, Mn, Ni and Mg show similar values in both systems, which is ascribed to lithological factors. The seasonal evolution of contaminants is typical of rivers affected by AMD, reaching a maximum in autumn due to the dissolution of evaporitic salts precipitated during the summer. Nevertheless, in the Tinto River, Ca, Na and Sr show a strong increase during the summer, probably due to a greater water interaction with marly materials, through which the last reach of the river flows. Ba has a different behaviour from the rest of metals and its concentration seems to be controlled by the solubility of barite. Fe, As and Pb show different behaviours in both rivers. Regarding Fe and As, this fact is possibly linked to different Fe dissolved species prevailing. The different Pb pattern is probably due to the control of Pb solubility by anglesite or other minerals rich in Pb in the Tinto River.

Key words: Tinto, Odiel, Ría of Huelva, AMD, metal pollution, hydrogeochemistry.

1. Introduction

The Tinto and Odiel Rivers drain materials from the Iberian Pyrite Belt (IPB), located in the southwest of the Iberian Peninsula (Fig.1). The IPB is rich in massive sulphide deposits, which have been exploited since 3000 BC for the extraction of gold, silver and copper (Nocete et al., 2005). In Roman times there was a resurgence of mining activity, whose traces remain throughout the IPB. Then, mining activity decreased, although it continued sporadically during Visigothic and Arab dominations and the Middle Ages. In the middle of XIX century, mining activity reappeared more intensively. Nearly one hundred mines have been active during XIX and XX centuries with a total output of 300 million tones of polymetallic ores (Sáez et al., 1999).

Currently, no active sulphur mine remains after closing the exploitations in Riotinto, Tharsis and Sotiel (Fig. 1), but residues of numerous exploitations keep producing acid leachates, which contaminate the Tinto and Odiel Rivers.

The Tinto River is a global extreme case of contamination by AMD (Lopez-Archilla and Amils, 1999; Amaral-Zettker et al., 2002; Fernández-Remolar et al., 2004). At its source, the river presents pH values close to 1 and then remain around pH 2.0 – 2.5 until its mouth in the Ría of Huelva. These characteristics are due to the pollution produced in the mining district of Riotinto, which covers an area around 20 km² and has a unique landscape with innumerable deserted mines, open-pits, dumps, tailing dams, etc. Most of the tributaries of the river are not affected by AMD, excluding those going through the Mining District. In the last few years, the Tinto River is being studied by its analogy with the extreme life conditions that could have existed in Mars (Fernández-Remolar et al., 2004 and 2005).

The Odiel River, although it does not show as extreme values as the Tinto River, is affected by numerous mines distributed along its basin, so most of the drainage network is affected by AMD (Sánchez-España et al., 2005; Sarmiento et al., 2005). The mines that produce a greater degradation of the river are the Mining District of Riotinto and the mining areas of Tharsis and Sotiel (Fig. 1). The contamination levels in the Odiel River near its mouth into the Ría of Huelva are much lower than in the Tinto. However, the contaminant load carried by the Odiel is larger due to its greater flow (Sáinz et al., 2004; Olías et al., 2006).

Although many studies devoted to the water quality of the Tinto and Odiel Rivers have been carried out, most of them are either based on sporadic samplings (e.g. López-Archilla y Amils, 1999; Hudson-Edwards et al., 1999; Ferris et al., 2004) or focused on the estuary (e.g. Elbaz-Poulichet et al., 2001; Achterberg et al., 2003; Braungardt et al., 2003). The aim of this study is to describe the hydrogeochemistry in both rivers from a systematic sampling, and try to explain the differences between them and the processes that control the contaminant concentration.

2. Study area

2.1. Geology

The IPB, whose dimensions are around 200 km long by 40 km wide, belongs to the South Portuguese Zone of the Hercynian Iberian Massif. It extends from the SW Spain to the Portuguese Atlantic coast.

The most southern part of the Tinto and Odiel basins runs through Neogene materials of the Guadalquivir depression. In this area, these materials are formed by marly deposits (Fig. 1). In the northern part of the area, some plutonic and metamorphic rocks of the Ossa-Morena Zone (Lower Precambrian to Paleozoic) outcrop.

The Iberian Pyrite Belt is formed by three lithological groups (Fig.1) belonging to the Upper Palaeozoic: 1) the Phyllite-Quartzite Group (PQ), formed by a thick sequence of shales and sandstones, 2) the Volcano-Sedimentary Complex (VSC), which includes a mafic-felsic volcanic sequence interstratified with shales, and 3) the Culm Group in which shales, sandstones and conglomerates prevail.

Associated with the materials of the Volcano-Sedimentary Complex, many massive sulphide sites are developed, with original reserves of 1,700 Mt (Sáez et al., 1999). The largest individual polymetallic sulphur deposit in the world, the mining district of Riotinto, is found among them. Pyrite (FeS_2) is the principal mineral in the massive sulphur deposits, with lower quantities of sphalerite (ZnS), galena (PbS), chalcopyrite (CuFeS_2), arsenopyrite (FeAsS) and other sulphurs with accessory quantities of Cd, Sn, Ag, Au, Co, Hg, etc.

2.2. Hydrology

The Tinto and Odiel Rivers have their source in the foothills of the Sierra de Aracena, over 900 m of height. The climate is of the mediterranean type, with rainy winters and dry, warm summers. The average pluviometry in their catchments varies between 600 mm in the lowest part in the south and over 1000 mm in the northern mountainous zone. The average temperature is near 18 °C.

The average Odiel discharge is close to 100 and 500 hm³/year in the Tinto and Odiel Rivers, respectively. Most of their courses flow over impermeable materials and, as a result, both rivers have a low natural regulation, their flow responds quickly to the rainfall and show strong variations, according to the pluviometric regime.

Both rivers flow into a common estuary, known as the Ría of Huelva (Fig.1), where many of the metals they transport precipitate due to the pH increase caused by the mixture with the sea water. As a result, sediments from the Ría of Huelva present very high metal concentrations (Ruiz et al., 1998; Leblanc et al., 2000; Borrego et al., 2002). Furthermore, the Ría receives contaminating inputs from an important industrial area located around the city of Huelva (Davis et al., 2000), although these contributions have decreased heavily over the last years.

The most mobile metals reach the Gulf of Cadiz (Fig. 1) producing very high contamination levels in the coast (Sáinz y Ruiz, 2006) and creating a contaminating plume which even enters in the Mediterranean Sea (van Geen et al., 1997; Elbaz Poulichet et al. 2001).

3. Methods

In February 2002, samplings in both rivers were started, with approximately a weekly periodicity. Samplings points are located before the rivers enter in the estuary (Fig. 1). In this study, results obtained until July 2005 —after three years and a half— are discussed.

Temperature, electrical conductivity, pH and redox potential were determined in the field with portable meters (HI 9025 and HI 9033). To measure the redox potential, a probe with a

platinum electrode and an Ag/AgCl reference electrode were used. The equipments were calibrated before carrying out the samplings. The redox potential was corrected in order to obtain the potential referred to the hydrogen electrode (Nordstrom and Wilde, 1998). Samples were filtrated (0.45 μm), cold preserved in pre-washed polyethylene containers and acidified with HNO_3 suprapur Merk® to $\text{pH} < 2$.

Analyses were carried out in the Central Research Services of the University of Huelva, by using a Jobin Yvon (JY ULTIMA 2) optical spectrometer (ICP-OES), equipped with a cyclonic concentric nebulizer. The method used was designed and contrasted in order to estimate major, minor and trace elements in waters affected by acid mine drainage (Ruiz et al., 2003; Tyler et al., 2004a and 2004b). It has been verified with certified reference material (SRM® NIST 1640) and interlab comparisons. The elements analysed are included in table 1, together with the concentration range and its detection limit. Samples out of range were diluted at a maximum dilution factor of 1:10.

Flow river data are obtained from two stream-gauging stations. The Odiel station is placed by the sampling location, whereas the Tinto station is located 9 km upstream from the sampling point. These stations have a poor operation and report frequent periods with no data.

4. Results and discussion

4.1. Comparison between both rivers

Results obtained during the study period (from February 2002 to July 2005) are shown in table 2. In the Tinto River, pH mean value was of 2.82 and usually ranged between 2.52 and 2.91 (percentiles 25 and 75), although it was closed to 5 during the floods. Eh mean value was of 723 mV and electrical conductivity of 2.49 mS/cm. Sulphates mean concentration was 1449 mg/L, with maximum values above 7400 mg/L. Regarding metals, Fe concentrations are the highest with a mean value of 151 mg/L and a maximum of 2804 mg/L. Al, Ca and Mg mean concentrations are close to 80 mg/L, followed by Na (39 mg/L), Zn (26 mg/L), Cu (19 mg/L), Mn (8 mg/L) and K (4 mg/L). Mean values of the rest of elements are below 1 mg/L.

The Odiel River shows a pH value slightly higher, with a mean value of 3.64 and usually ranged from 3.31 and 3.87 (percentiles 25 and 75). Eh is slightly lower to the Tinto value (652 mV). Electrical conductivity and sulphates content are around half of the values recorded in the Tinto River (mean of 1.21 mS/cm and 769 mg/L, respectively). Low Fe concentration (mean values of 8 mg/L) is remarkable compared to the values recorded in the Tinto River, although it has reached a maximum above 200 mg/L (Table 2). Other cations with mean concentrations over 1 mg/L are in decreasing order: Mg (mean value of 79 mg/L), Ca (52 mg/L), Al (41 mg/L), Na (20 mg/L), Zn (13 mg/L), Mn (9 mg/L), Fe (8 mg/L), Cu (6 mg/L) and K (3 mg/L).

The elements analysed from the greater to the lesser mean concentration values are shown in the following sketch. Those with concentration values above 1 mg/L are represented in bold and in italics those with concentration values below 0.1 mg/L.

TINTO RIVER

Fe>Al>Mg>Ca>Na>Zn>Cu>Mn>K > Co > Sr > Ni > As > Li > Pb > Cd > *Ba>Cr>Be*

ODIEL RIVER

Mg>Ca>Al>Na>Zn>Mn>Fe>Cu>K > Co>Ni>Sr > Li>Cd>Pb>Ba>As>Cr>Be

Apart from the different Fe concentration in both systems, As mean concentration is remarkable for its value of 160 µg/L in the Tinto River and only of 8 µg/L in the Odiel River, although these differences are reduced considering the median value (29 compared to 4 µg/L, respectively). Variation coefficients for As and Fe are much higher than for the rest of the elements in both rivers (Table 2). Other differences between both systems are the lowest Cu concentration (below Mn) and the greatest Ni concentration (above Sr) in the Odiel River.

Values showed in table 3 are obtained by dividing the mean values and medians of each element in the Tinto River by its value in the Odiel River. Al, Cd, Co, Li, Na, SO₄, Sr and Zn concentrations in the Tinto River are approximately twice as much as the concentrations in the Odiel River. On the contrary, Ba concentration is higher in the Odiel River, whereas Mg, Mn, Ni, and SiO₂ values are similar in both rivers. Fe concentration is approximately 20 times higher in the Tinto River, as well as As concentration (although As concentration is 6 times higher considering the median value). Cr, Cu and Pb contents in the Tinto River are more than double than those in the Odiel River.

Considering sulphates as conservatives (Berger et al. 2000; Sullivan and Drever, 2001), the Tinto River would receive, in relation to its discharge, twice as much contaminants as the Odiel River. When acid leachates mix with neutral waters non-affected by AMD, dissolved Fe suffers a process of hydrolysis and precipitates as ferric oxyhydroxisulphates. Therefore, dissolved Fe buffers the pH. In the Odiel River, the Fe buffer capacity is nearly exhausted,

due to a higher dissolution and natural self-treatment processes suffered by acid leachates. Hence the great differences in Fe concentration in both rivers.

This intense Fe precipitation in the drainage network of the Odiel River makes As concentrations low, very inferior to As concentrations in the Tinto River, since As is strongly sorpted and/or coprecipitated during the Fe oxyhydroxisulphates precipitation (Williams, 1999; Casiot et al., 2003). Cu also suffers a preferential precipitation in Fe oxyhydroxisulphates, as shown by Olías et al. (2004) for the Odiel River and Alpers et al. (1994) and Gray (1998) in other rivers affected by AMD. This fact would explain the lower Cu concentration in the Odiel River, which is three times lower than the Tinto concentration.

Pb can also suffer this coprecipitation process, more intense in the Odiel River, hence its relation between both rivers is above 2 (Table 3). Figure 2 points out that Cr is also affected by this coprecipitation process; more “evolved” waters which have suffered stronger processes of neutralisation, and thereby they have a minor Fe/SO₄ ratio, present less Cr concentration. On the other hand, leachates produced near the mining zones (greater Fe/SO₄) contain more Cr. This effect may be also valid for Pb, although in this case, correlation with Fe/SO₄ ratio is only significant for the Tinto River ($R=0.49$ $p<0.001$).

The concentrations of Mg, Mn, Ni and Be are similar in both rivers (Table 3). In relation to sulphates, their proportion is much higher in the Odiel river. This may be due to lithological factors, because of a greater abundance of Mn and Ni hydrothermal mineralizations in the Odiel basin (Cánovas et al., 2005a). Concerning Ba, it shows higher concentrations in the Odiel River, which is maybe due to a control of its solubility by barite, explained further on.

4.2. Time Evolution

Seasonal variation of the Odiel River concentrations has been studied by Ollas et al. (2004). During spring and summer, salinity increases progressively due to the strong evaporation, producing the soluble Fe oxyhydroxisulphates precipitation in the river courses and mining areas. Dissolution of these salts is produced with the first autumn rainfalls, when the highest contamination levels are reached. Once these salts are fully washed, contaminant concentrations decrease during the winter, due to the dilution caused by the highest river discharges. In spring and summer, concentrations increase again. This evolution is similar in the Tinto River, although there are several differences between both systems, as detailed below.

Over the study period, the discharge shows very sudden changes in response to precipitations (Fig. 3). Years 2001/02 and 2002/03 were more humid; in the Odiel River, where a more thorough data series is obtained, mean discharge was close to $20 \text{ m}^3/\text{s}$, whereas in 2003/04 was of $9 \text{ m}^3/\text{s}$ and in 2004/05, an extraordinarily dry year, below $1 \text{ m}^3/\text{s}$.

Figure 4 shows the evolution of some representative variables in both rivers. In the Odiel River there are no analytical data during the summer, as the water frequently stops flowing and gets stagnant. However, the Tinto River did not dry up at the control point, even though flows are very low, often below 10 L/s (Fig. 3).

pH evolution shows a minimum during the summer and higher values during the winter (Fig 4). Electrical conductivity shows a maximum during the first autumn rainfall, due to the evaporitic salts re-dissolution. During the autumn in 2002 there is a quite wide period with

high concentrations, whereas in 2003 and 2004 this period is narrower, reaching higher concentrations. This fact is due to the different precipitation distribution in both years. Thus, in October 2002 precipitations were only of 42 mm and the salt washing period went on until the middle of November, when intense rainfall occurred (100 mm during this month). However, in 2003 and 2004 October precipitations were of 180 and 140 mm, hence the washing of the salts accumulated during the summer was faster.

Sulphates, Al, Be, Cd, Co, Li, Mg, Ni and Zn evolution (not shown in the figure) is similar to the electrical conductivity variation. As regards Fe evolution, the wide variation range is remarkable (see log scale); the highest values are recorded during the autumn and the lowest values during the winter, where there are frequent peaks depending on the river flow. During the summer, Fe concentration remains stable and does not increase like the electrical conductivity and metals before mentioned. This indicates an intense Fe oxyhydroxisulphates precipitation during this time. The Fe/SO₄ ratio decreases during the summer, as shown in figure 5, due to a higher Fe precipitation and a more conservative behaviour of sulphates.

As evolution has a different behaviour from the rest of elements and shows lower values during the summer -especially in the Odiel River, where values are under the detection limit- because of the intense coprecipitation with Fe. In the Tinto River there is a maximum value, which coincides with the autumn washing, but it does not occur in the Odiel River.

Cr and Cu (not shown in the figure) show an evolution similar to Fe due to its tendency to coprecipitate with Fe oxyhydroxisulphates, though they have it has a minor variation range. However, this process is not as intense as for arsenic.

In the Tinto River, there is a strong increase of Sr (Fig. 4) as well as of Ca and Na (not shown) during the summer. This increase is much higher than for the rest of the elements, as shown in figure 6, where the evolution of Ca/Mg ratio is represented. This evolution can be due to the existence of Neogene marly materials in the controlled reach of the Tinto River (Fig. 1), which could have a stronger influence when the river flow is lower and there is a longer water contact with the riverbed materials.

Finally, Pb shows a slightly different behaviour to the rest of elements, with the maximum values recorded in autumn, but the highest peak does not occur simultaneously with the rest of metals, but a bit later on (Fig. 4). Furthermore, in the Tinto River, Pb concentration presents sudden peaks in spring, which are not observed in the rest of the analysed parameters.

4.3. Principal Component Analysis (PCA)

Considering the large amount of samples and variables analysed, a principal component analysis (PCA) of the results obtained for each river has been carried out. As some variables do not show a normal distribution, the Spearman's correlation matrix is used for the PCA (Davis, 1986). SiO₂ is not included since it was not determined in all the samples. For the Odiel River, Ba, Cr and Li are not included either because they were not analysed in several samples.

The first component (Fig. 7) describes most of the sample variance (68% in the Tinto River and 77% in the Odiel River). It is related to the sample salinity (sulphates, Al, Be, Cd, Co, Cr, Cu, Ni, Mg, Mn and Zn), whose variations are mainly controlled by the river flow variations (Olías et al., 2004; Cánovas et al., 2005b).

The second component explains a much lower percentage of the sample variance (15% and 9% in the Tinto and Odiel Rives, respectively). In the Tinto River this component is controlled by Sr, Na, Ca and K in the positive part, and by As, Fe and Pb in the negative side. In the Odiel River, it is mainly controlled by Fe and As concentrations (Fig. 7).

Ba has a different behaviour from most of the metals in the Tinto River (in the Odiel River is not included in the analysis). This behaviour seems to be due to the fact that Ba concentrations are controlled by the barite solubility, as discussed below. Therefore, when sulphates content decreases during the floods, Ba concentration can increase.

Pb behaviour is also remarkable in both rivers: in the Odiel it is associated to sulphates and most of metals, whereas in the Tinto River Pb is near to Fe and As (Fig.7). Figure 8 shows the very similar behaviour between Pb and Co (as well as the rest of elements located in the positive side of factor 1), whereas the correlation in the Tinto River is much worse.

Another difference between both systems lies in the relation between Fe and As and the elements located in the positive side of component 1: in the Odiel River, correlations are very low while they are high in the Tinto River (Fig.9). This fact can be due to the different concentrations of these elements in both rivers as well as to differences in the predominant Fe species, detailed below.

Moreover, in the Tinto River, componet 2 meets Fe, As and Pb on the one hand and K, Sr, Na and Ca on the other. This fact seems to be due to the seasonal evolution of both groups of elements. As already mentioned, during the summer Fe, As and Pb concentration is very low

(Fig. 4) due to the intense Fe oxyhydroxisulphates precipitation. At the same time, Sr (Fig 4) together with Ca, Na and K increase, due to a stronger interaction of the river water with the marly materials in the last reach of the river (Fig.1). In autumn and winter, on the contrary, Fe, As and Pb increase in connection with Ca, Na, Sr and K.

In the Odiel River, Ca and Na also seem to have an opposite behaviour to Fe and As in the second component (Fig.7), but it is not as obvious as in the Tinto River, since in this case the river does not cross through the Neogene marly materials (Fig.1).

4.4. Saturation Indices

A speciation analyses have been carried out using the PHREEQC code (Parkhurst and Appelo, 1999). Fe speciation shows interesting differences between both systems (Fig.10). In the Tinto River, FeSO_4^+ is by far the predominant species, while Fe(II) species (Fe^{2+} and FeSO_4) only represent 9% of the whole. On the other hand, in the Odiel River, species of Fe(II) represent 41% of the whole and moles of Fe^{2+} and FeSO_4^+ are approximately similar. This distribution can explain the differences between both systems (Fig. 7 and 9), due to Fe^{2+} is not as sensitive to pH increases as Fe^{3+} .

Figure 11 displays Box and Whisker diagrams showing the saturation index values of some common minerals, which can precipitate from mine acid waters. Barite (BaSO_4) is very close to saturation, which supports that Ba concentration is controlled by the solubility of barite. The converse relation between Ba and sulphates obtained in the PCA (Fig.7) also points out this control.

Gypsum ($\text{CaSO}_4 \cdot 2\text{H}_2\text{O}$), anglesite (PbSO_4) and celestine (SrSO_4) are slightly undersaturated, although their values in the Odiel River are slightly lower than in the Tinto River. Other sulphates such as melanterite ($\text{FeSO}_4 \cdot 7\text{H}_2\text{O}$) and epsomite ($\text{MgSO}_4 \cdot 7\text{H}_2\text{O}$) are highly undersaturated. However, this fact does not exclude the precipitation of these minerals in other river reaches closer to the mining area. For instance, melanterite, epsomite, gypsum and anglesite have been found in the Mining District of Riotinto and in the Tinto River banks (Hudson-Edwards et al., 1999; Buckby et al., 2003; Lottermoser, 2005). As the level of the river decreases in summer, pools can remain, in which salts concentrate by evaporation, reaching higher salinity levels than the river water.

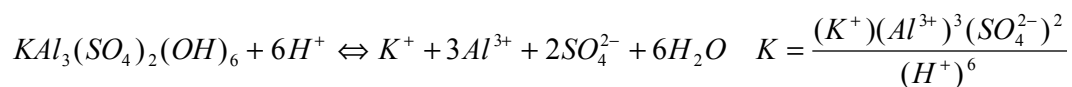
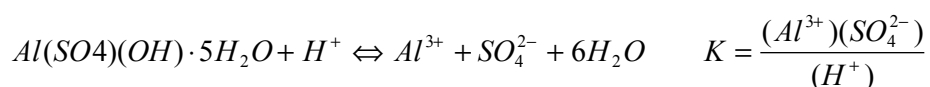
Figure 12 seems to indicate the existence of a control of Pb solubility by anglesite, though all samples are undersaturated at the samplings points; the upper limit is marked by saturation index (SI) equal to -1. This could be due to the fact that the control is carried out in a closer point to the mining area and new contributions of water not contaminated by AMD reduce the subsequent Pb and sulphates concentration. Hudson-Edwards et al. (1999) and Nieto et al. (2003) have shown that other jarosite group minerals, such as plumbojarosite and beudantite, can be important Pb 'sinks'.

Water is undersaturated in kaolinite ($\text{Al}_2\text{Si}_2\text{O}_5(\text{OH})_4$), like in other aluminosilicates. Oversaturated values can only be found in high floods, when pH rises. As usual in rivers affected by AMD, water is oversaturated in silica, as proved by chalcedony SI. Silica, contributed by aluminosilicates weathering, is a compound abundant in Fe oxyhydroxysulphates precipitates, as proved in data provided by Sánchez España et al. (2005).

High Al concentrations and low Fe contents in the Odiel River seem to show a pH control by Al, though the mean pH value found in the Odiel River (3.64) is slightly lower than in the values mentioned in the bibliography for systems buffered by Al.

Al minerals which can control its solubility in acid waters are jurbanite ($\text{Al}(\text{SO}_4)(\text{OH})\cdot 5\text{H}_2\text{O}$), alunite ($\text{KAl}_3(\text{SO}_4)_2(\text{OH})_6$), basaluminite ($\text{Al}_4(\text{SO}_4)(\text{OH})_{10}\cdot 5\text{H}_2\text{O}$) and microcrystalline gibbsite or amorphous $\text{Al}(\text{OH})_3$. Jurbanite is the most stable at low pH values (<4) and alunite, basaluminite and aluminium hydroxides would progressively take on special significance as the pH increases (Nordstrom and Alpers, 1999). Figure 10 does not show SI for basaluminite as values are extremely low and are out of the graphic scale. The Tinto River waters are clearly undersaturated in all of these minerals, apart from jurbanite, which shows slightly undersaturated values. In the Odiel River, every sample is slightly oversaturated in jurbanite, whereas alunite values are closer to equilibrium, but with a much higher variation range (Fig.10).

The dissolution reactions of jurbanite and alunite can be stated as follows:



where parenthesis indicates activities.

Due to the reaction stoichiometry, jurbanite saturation index depends less on the pH (it differs by one order of magnitude with a pH unity, whereas alunite differs by six orders of magnitude) and on the Al and sulphates activity (regarding jurbanite, both are raised to 1 in

calculations of the ionic activities product, whereas regarding alunite, Al is raised to 3 and sulphates to 2). This fact allows jurbanite to show a saturation index close to equilibrium in wide pH conditions. Nordstrom and Alpers (1999) and Blowes et al. (2004) point out that jurbanite, despite its apparent thermodynamic stability, is not important as Al solubility control in mining acid waters and this mineral barely precipitates in these environments.

Fe oxyhydroxyde-sulphates, which are formed from mining acid waters, due to its low crystallinity have been traditionally embraced as amorphous iron oxides or ferric hydroxides. These minerals are mainly formed by: K-jarosite ($\text{KFe}_3(\text{SO}_4)_2(\text{OH})_6$), ferrihydrite ($\text{Fe}(\text{OH})_3$), schwertmannite ($\text{Fe}_8\text{O}_8(\text{OH})_6(\text{SO}_4)$) and goethite (FeOOH). Jarosite is found in very acid environments, schwertmannite predominates over pH values between 3 and 4, and ferrihydrite and goethite are formed with pH values from 5 to 7 (Murad and Rojik, 2003). However, the solubility of these minerals is still being discussed due to its compositional variability, the instability of ferrihydrite and schwertmannite compounds which are quickly transformed into goethite, the presence of sulphates in the crystalline net and as adsorbed species, etc. (Yu et al., 1999).

In both rivers, the water is overaturated in goethite and slightly undersaturated in ferrihydrite. Regarding to K-jarosite, it is oversaturated in the Tinto River and close to equilibrium in the Odiel River. Nevertheless, saturation index in K-jarosite depends on the solubility constant used, which differs greatly according to different authors (Baron and Palmer, 1996). Hudson-Edwards et al. (1999) and Galán et al. (2003) have found jarosite in the sediments of the Tinto River.

Schwertmannite saturation indices have been calculated from the available K_e in the bibliography (Table 4). Bigham et al. (1996) and Yu et al. (1999) calculated K_e from the composition of natural acid waters at equilibrium with schwertmannite precipitates. Kawano and Tomita (2001) obtained K_e from data of a dissolution assay of schwertmannite precipitates taken from an acid spring. Majzlan et al. (2004) measured experimentally the enthalpy of formation of schwertmannite in the laboratory, by using calorimetry of acid solution from two synthetic samples.

SI values obtained by using K_e from Bigham et al. (1996) and Yu et al. (1999) are closer to equilibrium in both rivers, although they show a wide variation range due to the stoichiometry of the dissolution of this mineral (Table 4). The SI values obtained from Kawano and Tomita (2001) and Majzlan et al. (2004) have not been represented since they have a similar distribution than the previous ones although they are very oversaturated.

5. Conclusions

The Tinto and Odiel Rivers present high levels of contamination by AMD. Conditions in the Tinto River are more extreme, with a mean pH of 2.82 over the study period compared to 3.64 in the Odiel River. Concentrations of most of the contaminant elements in the Tinto River (sulphates, Al, Cd, Co, Li, Sr and Zn) are approximately twice the Odiel concentrations, which indicate that, related to its discharge, the Tinto River receives twice the contaminant load that the Odiel River.

In the Tinto River, Fe is the predominant metal, with mean values of 151 mg/L and maximum close to 3,000 mg/L, whereas in the Odiel River, Fe mean concentration is only of 8 mg/L. In the Odiel, most of Fe precipitates along the channel as a consequence of the greatest intensity of acidity neutralization processes. Cr, Cu and especially As coprecipitate with Fe, so that concentration of these elements in the Odiel is much lower than in the Tinto. This can also be valid for Pb, although its behaviour is more complex.

Be, Mg, Mn and Ni concentrations are approximately similar in both rivers. A greater proportion of these elements in the Odiel River can be due to lithological factors caused by the existence of many Mn and Ni mineralizations in its basin, associated to sulphur deposits.

The evolution of concentrations over the year is similar in both systems. Thus, the most conservative elements including sulphates, Al, Cd, Co, Li, Mn, Ni, and Zn, reach a maximum in autumn, a minimum in winter and a concentration recovery all through the spring and summer. However, Fe concentration does not increase during the summer due to a greater Fe oxyhydroxisulphates precipitation at that time, as the Fe/SO₄ ratio shows. As has an opposite behaviour, showing lower values in summer, due to its intense coprecipitation with Fe. Cu and Cr also show a similar evolution as Fe.

In the Tinto River, Ca, Sr and Na concentrations have strongly risen during low water. This fact is associated to a greater interaction of the river water with the marly materials in the last reach of the river where the sampling point is located.

PCA demonstrates that most of variance is related to the salinity, controlled by the river flow variations. Ba has a different behaviour to the rest of elements and increases as salinity

decreases. This fact seems to indicate that Ba concentration is controlled by barite solubility, and so it increases as sulphates concentration decreases. The analysis of saturation indices also supports this hypothesis, since barite presents a saturation index close to zero.

PCA also shows a different Fe and As behaviour in both systems, which can be due to the fact that Fe concentration is very low in the Odiel River. Moreover, in the Odiel River the Fe predominant species is Fe^{2+} , whereas in the Tinto River Fe^{2+} species are not important.

From PCA it may be deduced that Pb has a different behaviour in both systems; in the Odiel River its behaviour is very similar to sulphates and conservative metals (Al, Cd, Co, etc.), whereas in the Tinto River it is more alike to Ba behaviour. This fact could be due to Pb concentration control caused by the anglesite and jarosite group minerals (such as plumbojarosite and beudantite) in waters with high contents in this element. However, this control would not take place in the Odiel River as there are lower Pb concentrations.

The analysis of saturation indices shows that water is oversaturated in goethite and undersaturated in ferrihydrite in both systems. K-jarosite is oversaturated in the Tinto River and close to equilibrium in the Odiel River. Schwertmannite saturation index depends on the equilibrium constant (K_e) taken. Values closer to equilibrium are obtained by using the K_e calculated by Bigham et al. (1996) and Yu et al. (1999) from schwertmannite precipitation in natural systems affected by AMD.

In the Odiel River, due to low Fe concentrations and high Al concentrations, a pH control by the precipitation of any Al-mineral could arise. Jurbanite is very close to equilibrium, though

this balance can be apparent as shown by Nordstrom and Alpers (1999). If this control exists, it is more likely to be caused by alunite, which is close to equilibrium.

These conclusions are valid for both river reaches close to the mouth of the Ría of Huelva. Conditions in headwaters and middle reaches, closer to mines where leachates are produced, can be very different.

Acknowledgements

The authors wish to thank the Guadiana Hydrographic Confederation, and the Environmental Council of the Andalusia Regional Government for the information provided for this study, which has been financed through the project "Mining contamination evaluation, acid mine drainage treatment, hydrologic modelling of the Odiel river basin and study of the contaminant load to the Huelva estuary", financed by the Environmental Council of the Andalusia Regional Government, and REN2003-09590-C04-03 financed by the Spanish Ministry of Education and Science.

References

Achterberg EP, Herzl VMC, Braungardt CB, Millward, G.E. Metal behaviour in an estuary polluted by acid mine drainage: the role of particulate matter. *Environ Pollut* 2003 ; 121: 283-292.

- Alpers CN, Nordstrom DK, Thompson JM. Seasonal variations of Zn/Cu ratios in acid mine water from Iron Mountain, California. In: Alpers CN, Blowes DW, editors. *Environmental Geochemistry of Sulfide Oxidation*. American Chemical Society, New York, 1994, pp. 323-344.
- Amaral Zettler LA, Gómez F, Zettler E, Keenan BG, Amils R, Sogin ML. Eukaryotic diversity in Spain's river of fire. *Nature* 2002; 417: 137.
- Baron D, Palmer CD. Solubility of jarosite at 4-35 °C. *Geochim Cosmochim Acta* 1996; 60: 185-195.
- Berger AC, Bethke CM, Krumhansl JL. A process model of natural attenuation in drainage from a historic mining district. *Appl Geochem* 2000; 15: 655-666.
- Bigham JM, Schwertmann SJ, Traina S, Winland RL, Wolf M. Schwertmannite and the chemical modelling of iron in acid sulfate waters. *Geochim Cosmochim Acta* 1996; 60: 2111-2121.
- Blowes DW, Ptacek CJ, Jambor JL, Weisener CG. The geochemistry of acid mine drainage. In: Lollar BS, editor, *Treatise on Geochemistry*, vol. 9 *Environmental Geochemistry*, Elsevier Ltd., Oxford, 2004, pp. 205-262.
- Borrego J, Morales JA, de la Torre ML, Grande JA. Geochemical characteristics of heavy metal pollution in surface sediments of the Tinto and Odiel river estuary (southwestern Spain). *Environ Geol* 2002; 41: 785-796.
- Braungardt CB, Achterberg EP, Elbaz-Poulichet F, Morley NH. Metal geochemistry in a mine-polluted estuarine system in Spain. *Appl Geochem* 2003; 18: 1757-1771.
- Buckby T, Black S, Coleman ML, Hodson ME. Fe-sulphate-rich evaporative mineral precipitates from the Río Tinto, southwest Spain. *Mineral Mag* 2003; 67: 263-278.

Cánovas CR, Olías M, Sarmiento AM, Nieto JM. Evolución temporal de la calidad del agua en los ríos Tinto y Odiel. In: López-Geta JA, Rubio-Campos JC, Martín-Machuca M, editors, VI Simposio del Agua en Andalucía, Seville, Spain, 2005a; II: 1309-1319.

Cánovas CR, Hubbard C, Olías M, Nieto JM, Black S, Coleman M. Water quality variations in the Tinto River during high flood events. In: Loredó J, Pendás F, editors. 9th International Mine Water Association Congress, Oviedo, Spain, 2005b; 133-139.

Casiot C, Morin G, Juillot F, Bruneel O, Personné JC, Leblanc M, Duquesne K, Bonnefoy V, Elbaz-Poulichet F. Bacterial immobilization and oxidation of arsenic in acid mine drainage (Carnoulès creek, France). *Water Res* 2003; 37: 2929-2936.

Davis JC. *Statistical and data analysis in geology*. John Wiley & Sons. Singapore, 1986, 646 pp.

Davis RA, Welty AT, Borrego J, Morales JA, Pendon JG, Ryan JG. Rio Tinto estuary (Spain): 5000 years of pollution. *Environ Geol* 2000; 39: 1107-1116.

Elbaz-Poulichet F, Braungardt C, Achterberg E, Morley N, Cossa D, Beckers JM, Nomérange P, Cruzado A, Leblanc M. Metal biogeochemistry in the Tinto-Odiel rivers (Southern Spain) and in the Gulf of Cadiz: a synthesis of the results of TOROS project. *Cont Shelf Res* 2001; 21: 1961-1973.

Fernández-Remolar D, Gómez-Elvira J, Gómez F, Sebastián E, Martín J, Manfredi JA, Torres J, González Kesler A, Amils R. The Tinto River, an extreme acidic environment under control of iron, as an analog of the *Terra Meridiani* hematite site of Mars. *Planet Space Sci* 2004; 52: 239-248.

Fernández-Remolar DC, Morris RV, Gruener JE, Amils R, Knoll, A. The Rio Tinto Basin, Spain: Mineralogy, sedimentary geobiology, and implications for interpretation of outcrop rocks at Meridiana Planum, Mars. *Earth Planet Sci Letters* 2005; 240: 149-167.

- Ferris FG, Hallbeck L, Kennedy CB, Pedersen K. Geochemistry of acidic Rio Tinto headwaters and role of bacteria in solid phase metal partitioning. *Chem Geol* 2004; 212: 291-300.
- Galán E, Gómez-Ariza JL, González I, Fernández-Caliani JC, Morales E, Giráldez I. Heavy metal partitioning in river sediments severely polluted by acid mine drainage in the Iberian Pyrite Belt. *Appl Geochem* 2003; 18: 409-421.
- Gray NF. Acid mine drainage composition and the implications for its impact on lotic systems. *Water Res* 1998; 32: 2122-2134.
- Hudson-Edwards KA, Schell C, Macklin MG. Mineralogy and geochemistry of alluvium contaminated by metal mining in the Rio Tinto area, southwest Spain. *Appl Geochem* 1999; 14: 1015-1030.
- Kawano M, Tomita K. Geochemical modelling of bacterially induced mineralization of schwertmannite and jarosite in sulfuric acid spring water. *Am Mineral* 2001; 86: 1156-1165.
- Leblanc M, Morales JA, Borrego J, Elbaz-Poulichet F. 4,500-year-old mining pollution in southwestern Spain: long-term implications for modern mining pollution. *Economic Geol* 2000; 95: 655-662.
- López-Archilla AI, Amils R. A comparative ecological study of two acidic rivers in southwestern Spain. *Microb Ecol* 1999; 38: 146-156.
- Lottermoser BG. Evaporative mineral precipitates from a historical smelting slag dump, Río Tinto, Spain. *N. Jb. Miner. Abh.* 2005; 181/2: 183-190.
- Majzlan J, Navrotsky A, Schwertmann U. Thermodynamics of Iron Oxides: Part III. Enthalpies of Formation and Stability of Ferrihydrite ($\sim\text{Fe}(\text{OH})_3$), Schwertmannite ($\sim\text{FeO}(\text{OH})_{3/4}(\text{SO}_4)_{1/8}$), and $\epsilon\text{-Fe}_2\text{O}_3$. *Geochim Cosmochim Acta* 2004; 68: 1049-1059.

Murad E, Rojik P. Iron-rich precipitates in a mine drainage environment: Influence of pH on mineralogy. *Am Mineral* 2003; 88: 1915-1918.

Nieto JM, Capitán MA, Sáez R, Almodóvar GR. Beudantite: a natural sink for As and Pb in sulphide oxidation processes. *Appl Earth Sci (T. I. Min. Metall. B.)* 2003; 112: 293-296.

Nocete F, Alex E, Nieto JM, Sáez R, Bayona MR. An archaeological approach to regional environmental pollution in the south-western Iberian Peninsula related to Third millenium BC mining and metallurgy. *J Archaeological Sci* 2005; 32: 1566-1576.

Nordstrom DK, Wilde FD. Reduction-oxidation potencial (electrode method). In: National field manual for the collection of water quality data. U.S. Geological Survey Techniques of Water-Resources Investigations, book 9, 1998, chapter 6.5.

Nordstrom DK, Alpers CN. Geochemistry of acid mine waters. In: Plumlee GS, Logson MJ, editors. The environmental geochemistry of mine waters. *Rev Econ Geol* 1999; 6A: 133-160.

Olías M, Nieto JM, Sarmiento AM, Cerón JC, Cánovas CR. Seasonal water quality variations in a river affected by acid mine drainage: the Odiel River (South West Spain). *Sci Total Environ* 2004 ; 333: 267-281.

Olías M, Cánovas CR, Nieto JM, Sarmiento AM. Evaluation of the dissolved load transported by the Tinto and Odiel rivers (South West Spain). *Appl Geochem* 2006 (in press).

Parkhurst DL, Appelo CAJ. User's guide to PHREEQC (Version 2) - A computer program for speciation, batch reaction, one-dimensional transport, and inverse geochemical calculations. USGS Water-Resources Investigations Report 99-4259. Denver, 1999, 312 pp.

Ruiz F, González-Regalado ML, Borrego J, Morales JA, Pendón JG, Muñoz JM. Stratigraphic sequence, elemental concentrations and heavy metal pollution in Holocene sediments from the Tinto-Odiel Estuary, southwestern Spain. *Environ Geol* 1998; 34: 270-278.

Ruiz MJ, Carrasco R, Pérez R, Sarmiento AM, Nieto JM, 2003. Calibración de un estándar natural para el análisis de muestras de drenaje ácido de minas (AMD) mediante UN-ICP-OES. IV Iberian Geochemical Meeting, 14-18 July, Coimbra, Portugal, 2003, pp. 414-416.

Sáez R, Pascual E, Toscano M, Almodóvar GR. The Iberian type of volcano-sedimentary massive sulphide deposits. *Miner Deposita* 1999; 34: 549-570.

Sáinz A, Grande JA, de la Torre ML. Characterisation of heavy metal discharge into the Ría of Huelva. *Environ Int* 2004; 30: 557-566.

Sáinz A, Ruiz F. Influence of the very polluted inputs of the Tinto-Odiel system on the adjacent littoral sediments of southwestern Spain: A statistical approach. *Chemosphere* 2006; 62: 1612-1622.

Sánchez España J, López Pamo E, Santofimia E, Aduvire O, Reyes J, Baretino D. Acid mine drainage in the Iberian Pyrite Belt (Odiel river watershed, Huelva, SW Spain): Geochemistry, mineralogy and environmental implications. *Appl Geochem* 2005; 20: 1320-1356.

Sarmiento AM, Nieto JM, Olías M, Cánovas CR. Environmental impact of mining activities in the Odiel river basin (SW Spain). In: Loredó J, Pendás F, editors. 9th International Mine Water Association Congress, Oviedo, Spain, 2005, pp. 89-94.

Sullivan AB, Drever JI. Geochemistry of suspended particles in a mine-affected mountain stream. *Appl Geochem* 2001; 16: 1663-1676.

Tyler G, Carrasco R, Nieto JM, Pérez R, Ruiz MJ, Sarmiento AM. Optimization of major and trace element determination in acid mine drainage samples by ultrasonic nebulizer-ICP-OES (USN-ICP-OES). Pittcon 2004 Conference, Chicago, 2004, CD-ROM, Abst. # 9000-1000.

Tyler G, Dubuisson C, Ruiz MJ, Carrasco R, Sanchez-Rodas D, Pérez R, Sarmiento AM, Nieto JM. Optimization of major and trace element determination in acid mine drainage water samples by USN-ICP-OES. 2004b, CETAC Technologies Application Notes, "U-5000AT+": http://www.cetac.com/anotes/appnotespdf/U5000_MineDrainagePoster.pdf

van Geen A, Adkins JF, Boyle EA, Nelson CH, Palanques A. A 120 yr record of widespread contamination from mining of the Iberian pyrite belt. *Geol* 1997; 25: 291-294.

Williams M. Arsenic in mine waters: an international study. *Environ Geol* 1999; 40: 267-278.

Yu JY, Heo B, Choi IK, Cho JP, Chang HW. Apparent solubilities of schwertmannite and ferrihydrite in natural stream waters polluted by mine drainage. *Geochim Cosmochim Acta* 1999; 63: 3407-3416.

FIGURE CAPTIONS.

Figure 1. Tinto and Odiel Rivers location map, indicating geology, main mines and sampling points.

Figure 2. Relationship between Cr and Fe/SO₄ in both rivers.

Figure 3. Evolution of river flow in both rivers from September 2001 to August 2005. The thick, horizontal line indicates periods with no data.

Figure 4. Evolution of pH, electrical conductivity (EC) and Fe and As concentrations in both rivers.

Figure 5. Evolution of Sr and Pb concentrations in both rivers.

Figure 6. Evolution of Fe/SO₄ and Ca/Mg ratios in both Rivers.

Figure 7. Results obtained from PCA in both rivers.

Figure 8. Relationship between Pb and Co in both rivers.

Figure 9. Electrical conductivity (EC) versus Fe and Al versus As in both rivers.

Figure 10. Main iron species in both rivers.

Figure 11. Box and Whisker diagrams of some minerals saturation indices obtained for both rivers.

Figure 12. Relationship between SO₄ and Pb activities in both rivers.

TABLE INDEX

Table 1. Elements analysed, concentration range and detection limit (DL).

Table 2. Results obtained in the Tinto and Odiel Rivers (February 2002-July 2005).

Table 3. Relation between mean values and medians of every element in the Tinto River divided by the equivalent values in the Odiel River.

Table 4. Data from the schwertmannite balance constant given by several authors.

Figure 1
[Click here to download high resolution image](#)

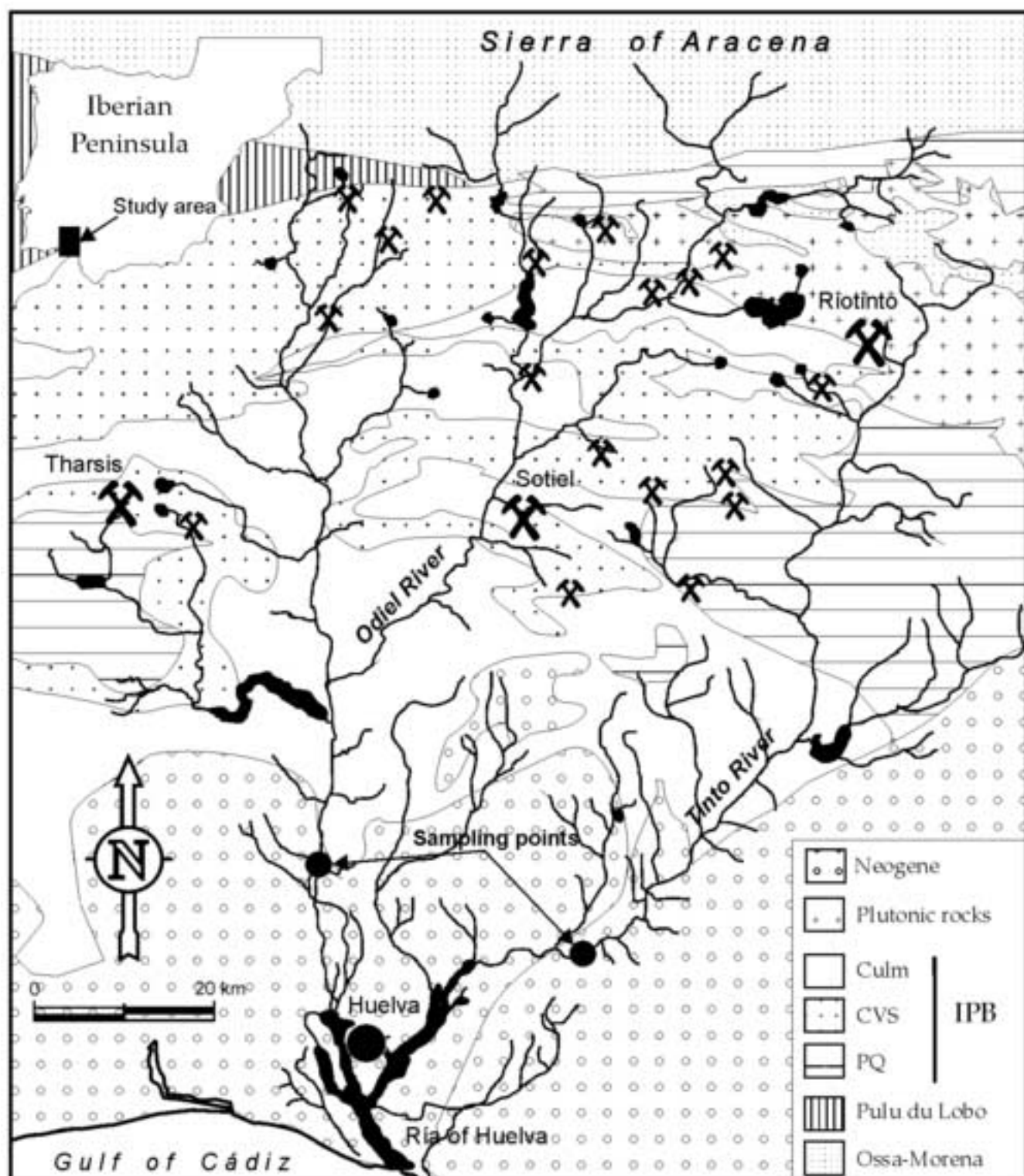


Figure 2
[Click here to download high resolution image](#)

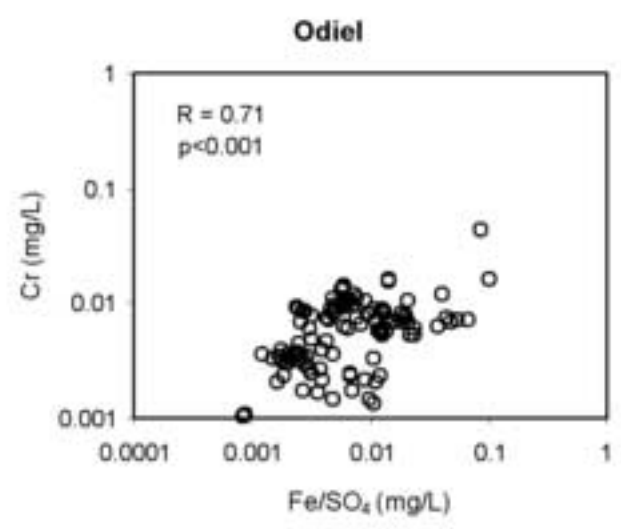
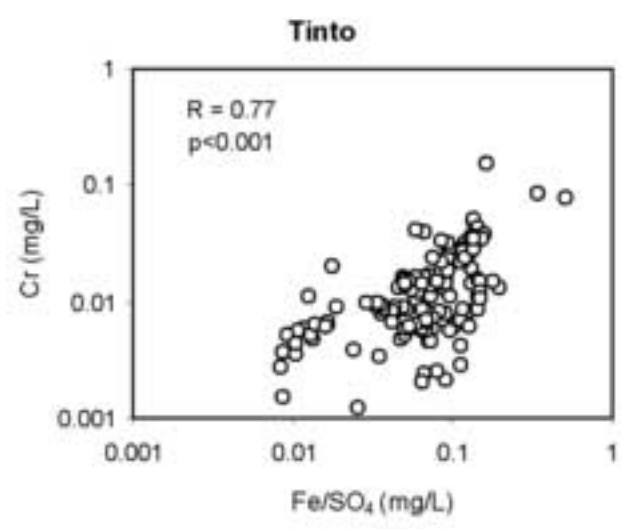


Figure 3
[Click here to download high resolution image](#)

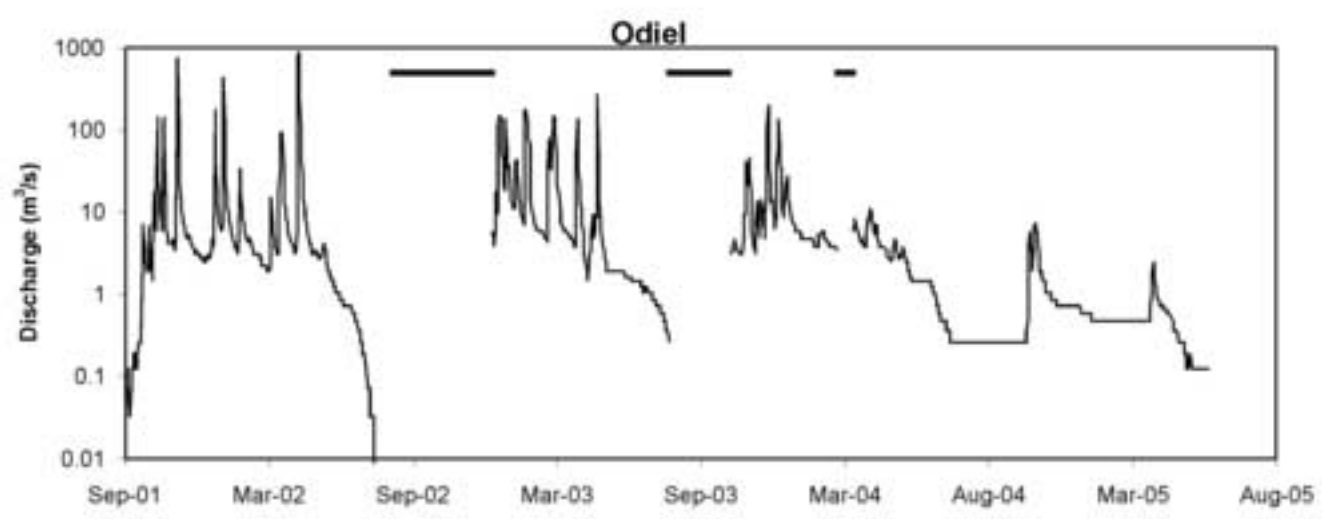
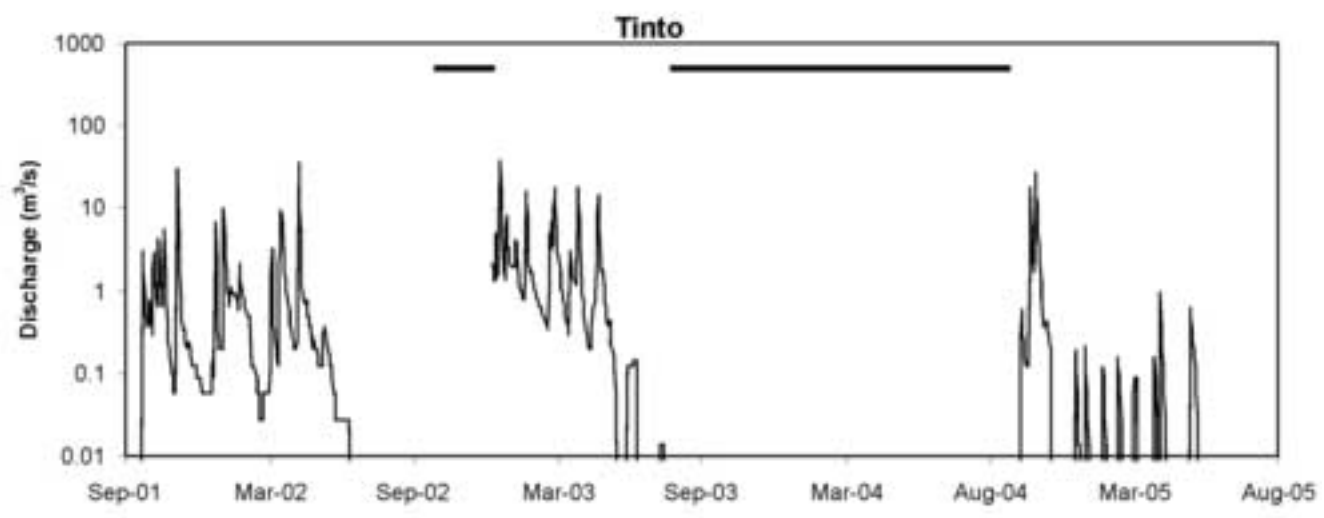


Figure 4

[Click here to download high resolution image](#)

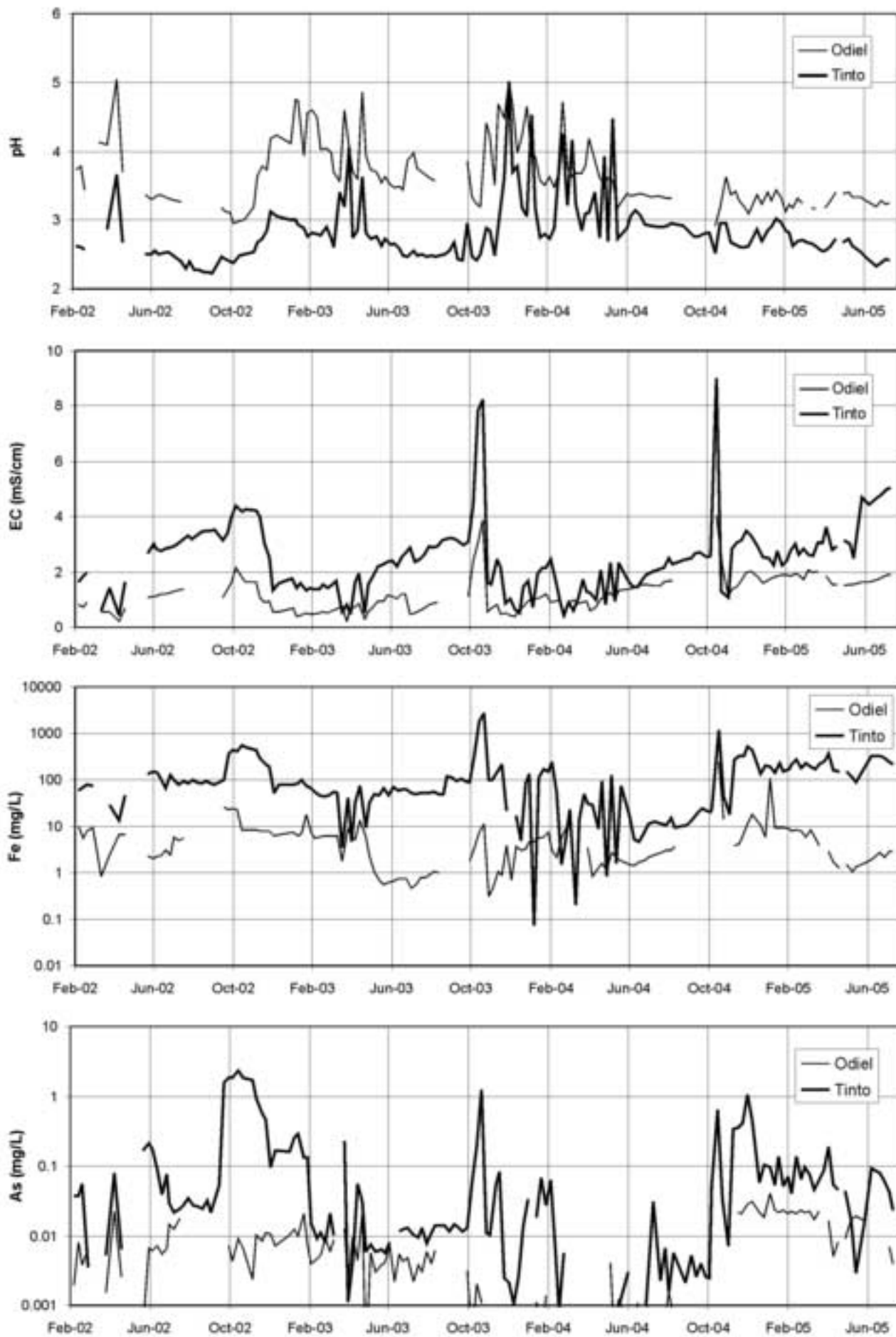


Figure 5
[Click here to download high resolution image](#)

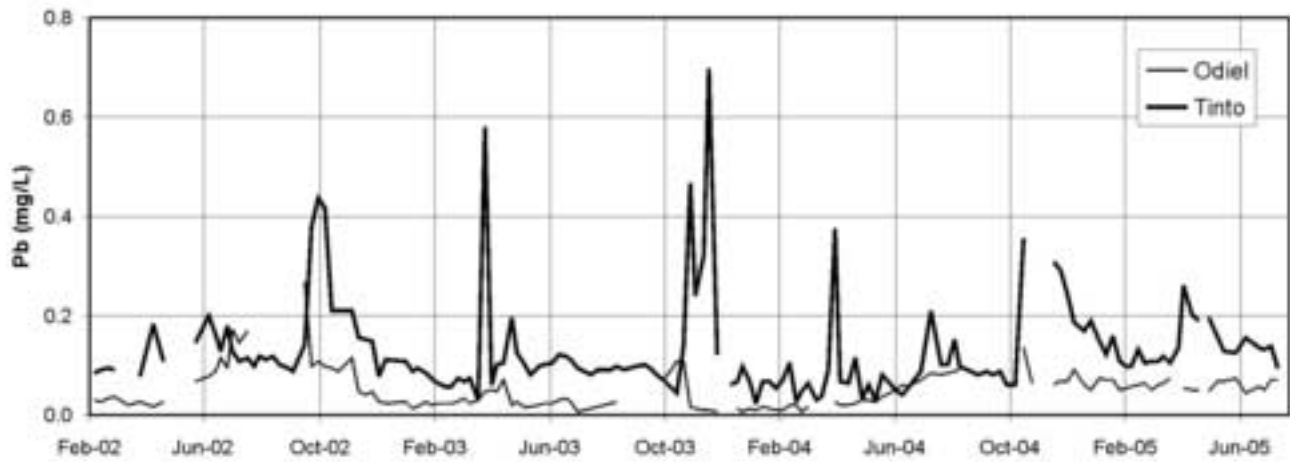
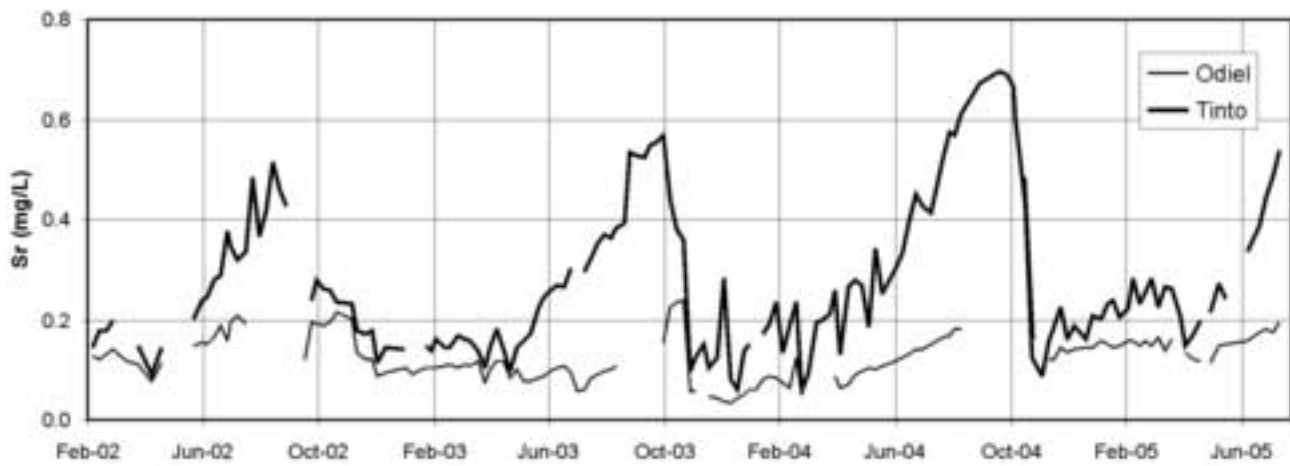


Figure 6
[Click here to download high resolution image](#)

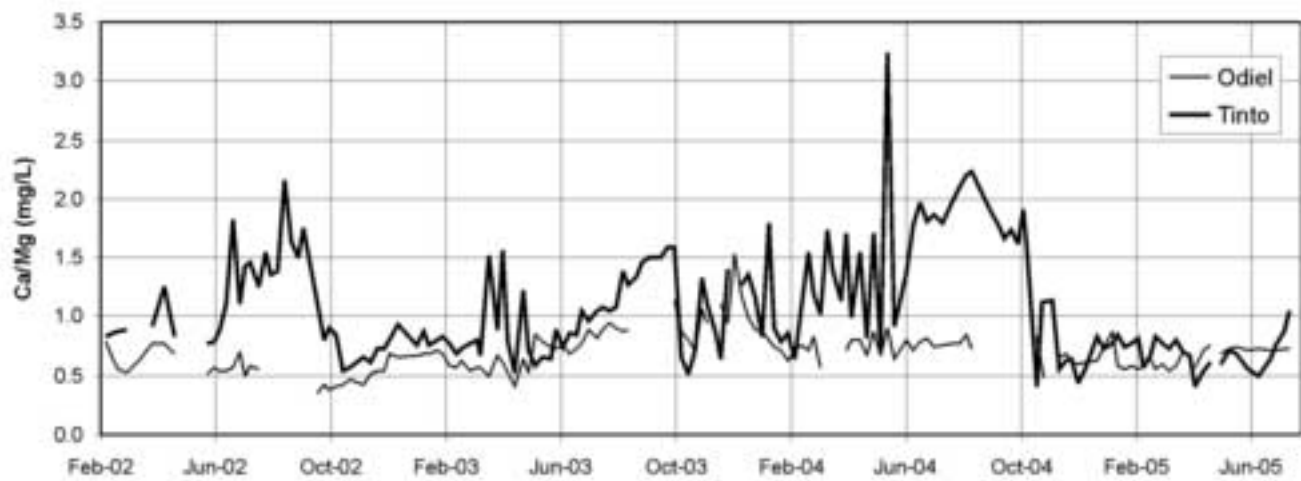
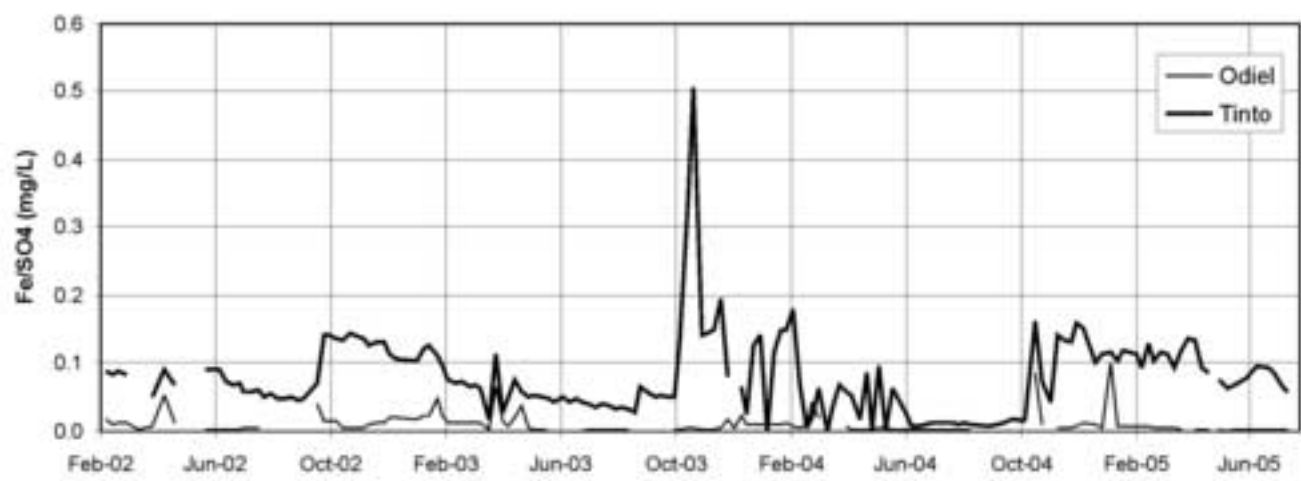


Figure 7
[Click here to download high resolution image](#)

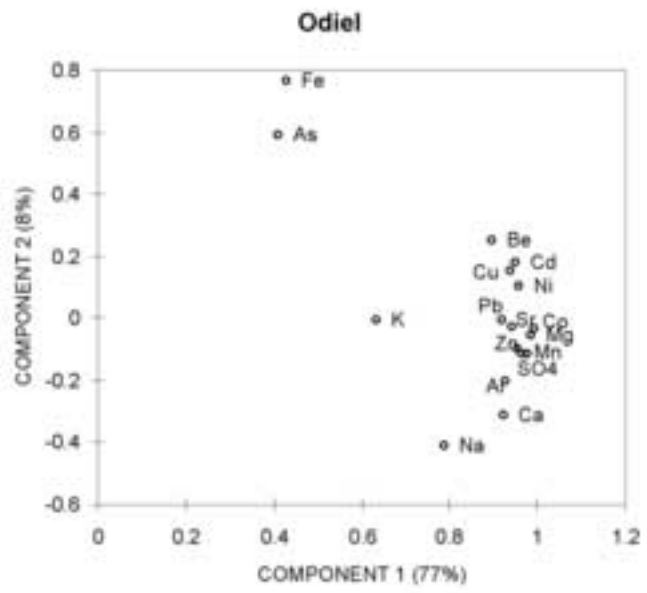
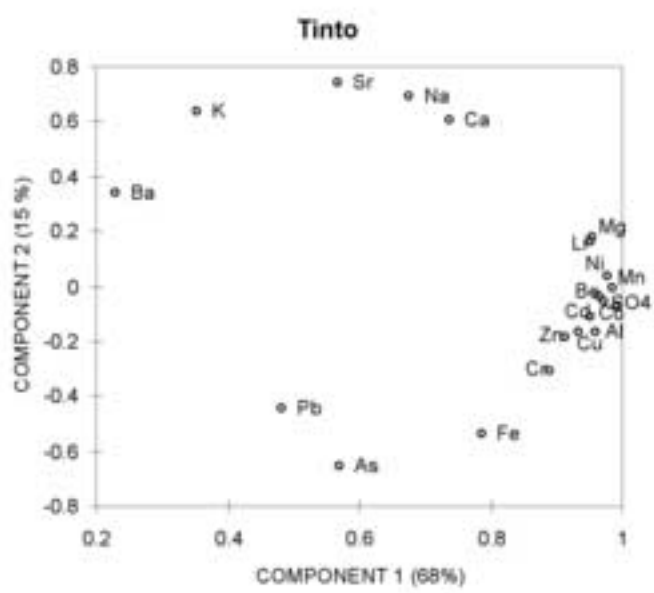


Figure 8
[Click here to download high resolution image](#)

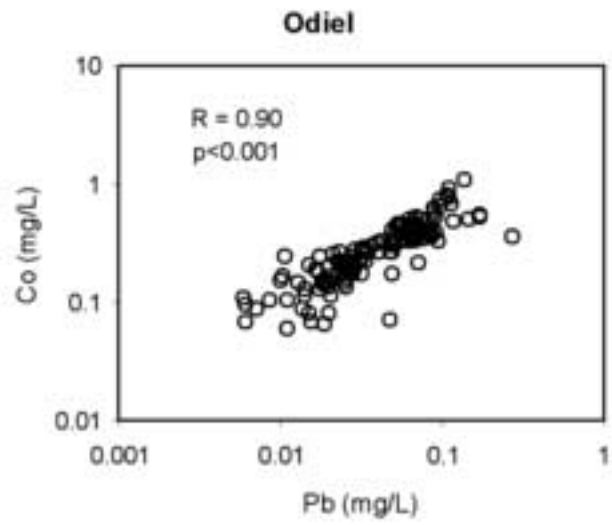
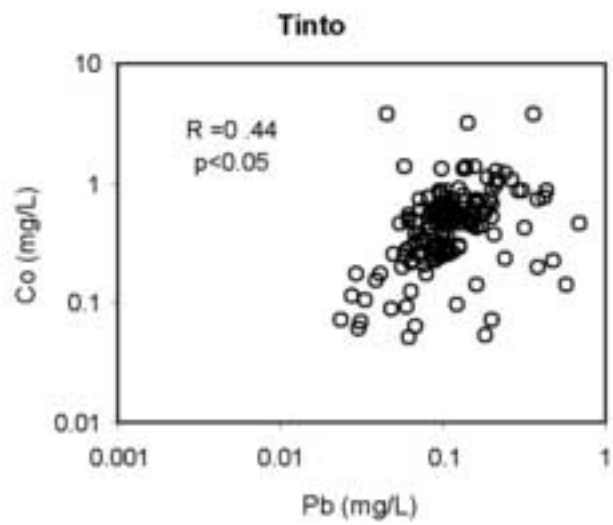


Figure 9

[Click here to download high resolution image](#)

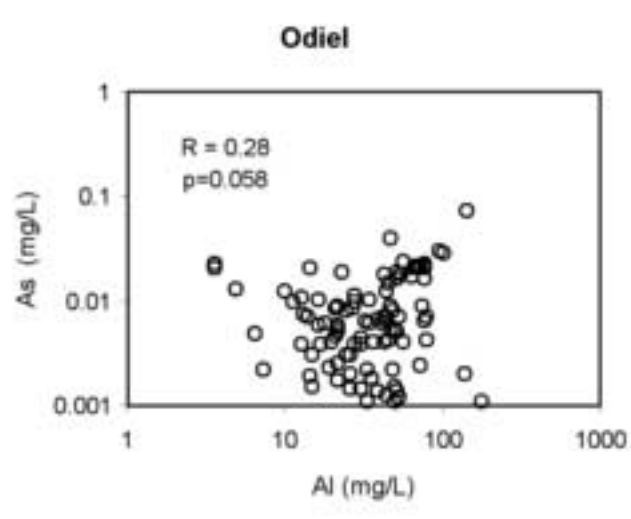
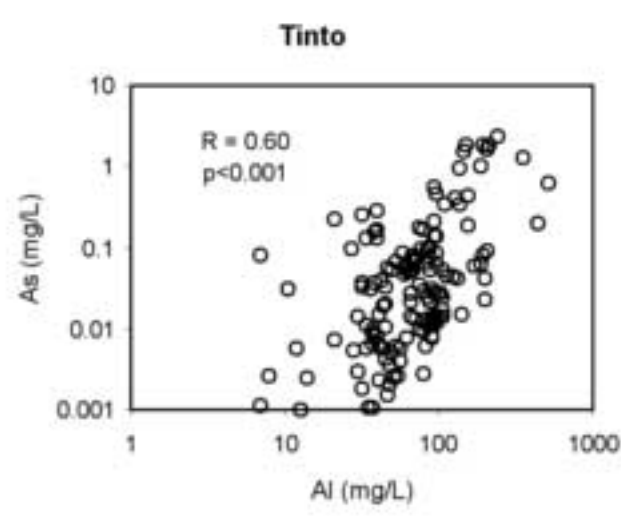
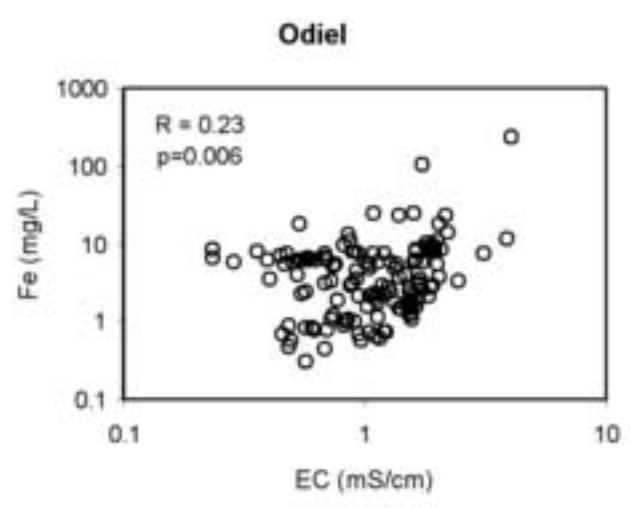
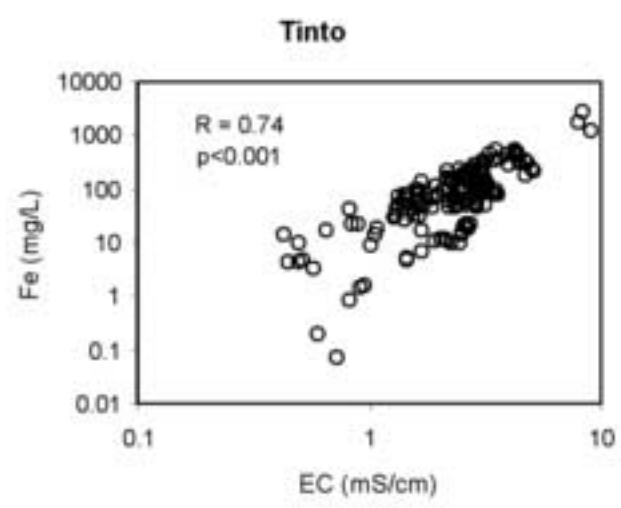


Figure 10
[Click here to download high resolution image](#)

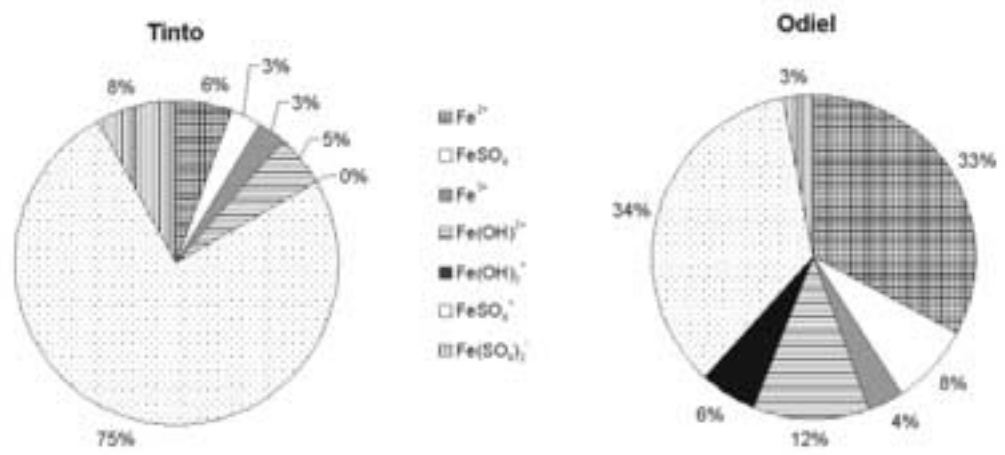


Figure 11
[Click here to download high resolution image](#)

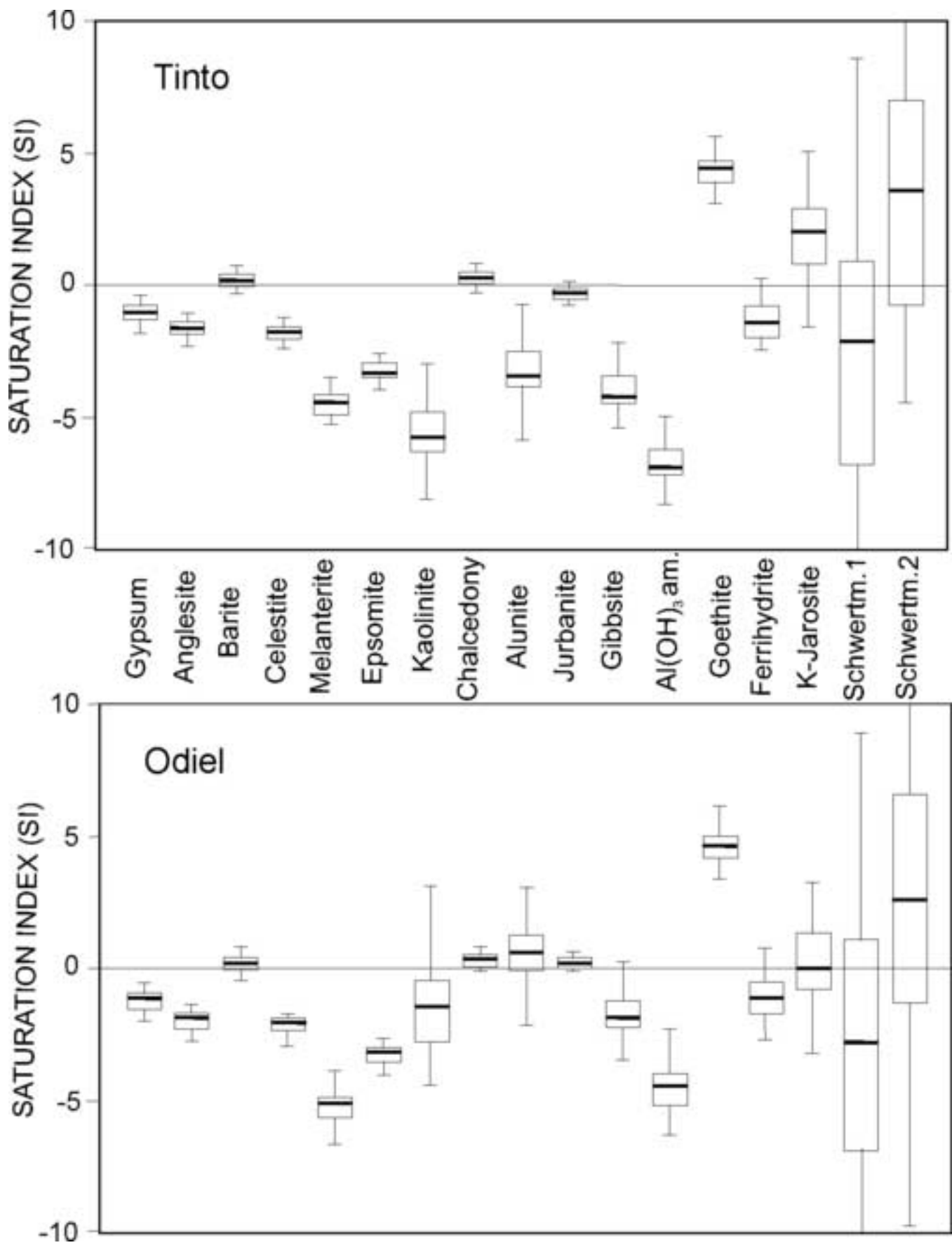


Figure 12
[Click here to download high resolution image](#)

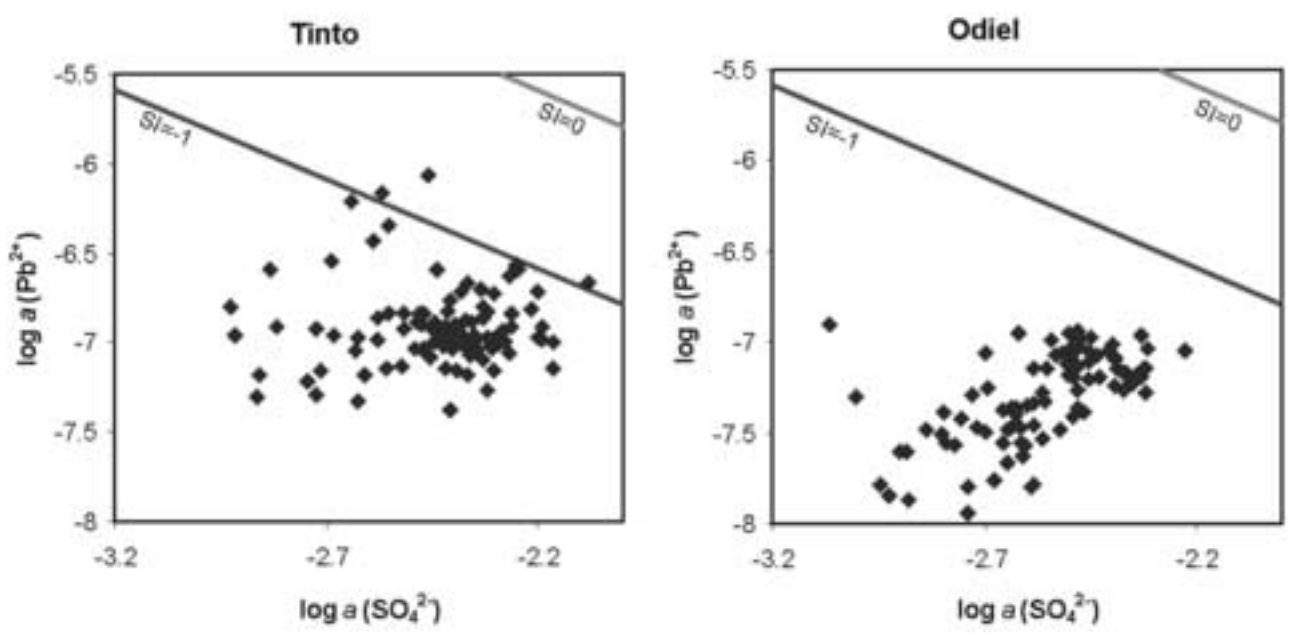


Table 1[Click here to download Table: Table01.xls](#)

Element	Range	D.L.
Al (mg/L)	0-200	0.06
As (µg/L)	0-4000	2.7
Ba (µg/L)	0-5000	0.2
Be (µg/L)	0-1000	0.1
Ca (mg/L)	0-200	0.006
Cd (µg/L)	0-2000	0.3
Co (µg/L)	0-4000	1.9
Cr (µg/L)	0-2000	1.7
Cu (mg/L)	0-20	0.001
Fe (mg/L)	0-200	0.003
K (mg/L)	0-20	0.056
Li (µg/L)	0-1000	1.5
Mg (mg/L)	0-200	0.0001
Mn (mg/L)	0-10	0.0003
Na (mg/L)	0-50	0.018
Ni (µg/L)	0-2000	1.2
Pb (µg/L)	0-4000	7
S (mg/L)	0-800	0.003
Si (mg/L)	0-20	0.008
Sr (µg/L)	0-3000	0.07
Zn (mg/L)	0-50	0.14

Table 2

[Click here to download Table: Table02.xls](#)

		TINTO RIVER							
		Mean	Minimum	Maximum	S.D.	V. C.	Median	Perc. 25	Perc. 75
Temp.	°C	19.6	6.3	33.0	6.8	35%	20.0	13.1	25.9
pH		2.82	2.22	5.01	0.45	16%	2.73	2.52	2.91
Eh	mV	723	456	816	68	9%	742	693	765
E.C.	mS/cm	2.49	0.43	9.00	1.30	53%	2.48	1.62	3.03
Al	mg/L	78.7	0.03	507.8	69.5	88%	65.2	37.4	94.1
As	mg/L	0.160	<0.003	2.290	0.395	247%	0.029	0.008	0.084
Ba	mg/L	0.017	0.005	0.080	0.013	76%	0.014	0.009	0.019
Be	mg/L	0.003	0.0003	0.022	0.003	80%	0.003	0.002	0.004
Ca	mg/L	76.6	11.1	228.0	50.0	65%	62.4	38.9	100.3
Cd	mg/L	0.118	0.011	0.680	0.090	76%	0.100	0.065	0.152
Co	mg/L	0.564	0.052	3.754	0.513	91%	0.491	0.274	0.656
Cr	mg/L	0.016	<0.002	0.158	0.018	114%	0.010	0.006	0.019
Cu	mg/L	18.9	0.2	133.9	15.4	82%	16.3	10.0	23.2
Fe	mg/L	151	0.07	2804	290	192%	81	42	162
K	mg/L	4.0	0.6	23.6	3.0	75%	3.3	2.2	4.9
Li	mg/L	0.135	0.009	0.754	0.100	74%	0.123	0.055	0.184
Mg	mg/L	77.4	8.9	451.3	59.8	77%	70.7	37.6	93.5
Mn	mg/L	8.0	0.7	54.7	6.5	82%	7.6	3.8	9.7
Na	mg/L	39.7	6.7	98.3	22.2	56%	35.9	21.8	53.7
Ni	mg/L	0.170	0.016	1.260	0.146	86%	0.145	0.075	0.207
Pb	mg/L	0.130	<0.007	0.698	0.098	76%	0.101	0.080	0.145
SO ₄	mg/L	1449	151	7434	1056	73%	1300	711	1770
SiO ₂	mg/L	35.3	2.8	133.4	23.4	66%	27.6	17.8	49.1
Sr	mg/L	0.280	0.060	0.696	0.153	55%	0.237	0.162	0.362
Zn	mg/L	26.0	2.2	152.3	22.4	86%	21.7	14.4	33.9

		ODIEL RIVER							
		Mean	Minimum	Maximum	S.D.	V. C.	Median	Perc. 25	Perc. 75
Temp.	°C	19.1	7.8	29.6	6.3	33%	19.5	12.9	25.2
pH		3.64	2.92	5.05	0.47	13%	3.51	3.31	3.87
Eh	mV	652	456	804	58	9%	658	629	688
E.C.	mS/cm	1.21	0.24	4.05	0.63	52%	1.11	0.73	1.61
Al	mg/L	40.7	0.6	175.8	29.1	71%	34.8	20.3	52.7
As	mg/L	0.008	<0.003	0.073	0.010	126%	0.004	0.001	0.011
Ba	mg/L	0.021	0.004	0.051	0.008	39%	0.022	0.015	0.027
Be	mg/L	0.003	0.0001	0.008	0.002	49%	0.003	0.002	0.004
Ca	mg/L	51.7	11.9	161.0	25.8	50%	48.6	32.5	67.7
Cd	mg/L	0.057	0.005	0.191	0.036	63%	0.052	0.030	0.073
Co	mg/L	0.308	0.033	1.073	0.184	60%	0.283	0.172	0.389
Cr	mg/L	0.006	<0.002	0.043	0.005	93%	0.005	0.002	0.008
Cu	mg/L	6.1	0.5	35.7	4.0	66%	5.6	3.8	7.6
Fe	mg/L	7.6	0.3	235.6	21.9	289%	3.8	1.8	7.6
K	mg/L	2.6	0.2	22.0	2.3	87%	2.3	1.6	2.9
Li	mg/L	0.077	0.005	0.354	0.050	66%	0.065	0.038	0.110
Mg	mg/L	79.1	10.1	224.1	43.6	55%	71.7	46.2	104.7
Mn	mg/L	9.0	0.9	32.1	5.8	64%	7.8	4.6	11.7
Na	mg/L	20.1	7.9	72.6	7.9	39%	18.6	14.5	25.2
Ni	mg/L	0.163	0.019	0.500	0.108	66%	0.144	0.080	0.227
Pb	mg/L	0.050	<0.007	0.267	0.039	77%	0.041	0.022	0.070
SO ₄	mg/L	769	110	2708	443	58%	693	450	1032
SiO ₂	mg/L	34.0	10.4	90.4	18.4	54%	28.0	19.5	44.3
Sr	mg/L	0.126	0.034	0.484	0.054	43%	0.119	0.091	0.154

Zn	mg/L	13.1	1.3	41.7	7.3	56%	12.9	7.5	17.0
-----------	------	------	-----	------	-----	-----	------	-----	------

Table 3[Click here to download Table: Table03.xls](#)

	Mean	Median		Mean	Median
Al	1.9	1.9	Li	1.8	1.9
As	20.2	6.5	Mg	1.0	1.0
Ba	0.8	0.6	Mn	0.9	1.0
Be	1.0	0.9	Na	2.0	1.9
Ca	1.5	1.3	Ni	1.0	1.0
Cd	2.1	1.9	Pb	2.6	2.4
Co	1.8	1.7	SO₄	1.9	1.9
Cr	2.8	1.8	SiO₂	1.0	1.0
Cu	3.1	2.9	Sr	2.2	2.0
Fe	19.9	21.5	Zn	2.0	1.7
K	1.5	1.5			

Table 4[Click here to download Table: Table04.xls](#)

Authors	Reaction	log K _e
Bigham et al. (1996)	$\text{Fe}_8\text{O}_8(\text{OH})_{4.8}(\text{SO}_4)_{1.6} + 20.8\text{H}^+ \leftrightarrow 8\text{Fe}^{3+} + 1.6\text{SO}_4^{2-} + 12.8 \text{H}_2\text{O}$	18.0±2.5
Yu et al. (1999)	$\text{Fe}_8\text{O}_8(\text{OH})_{4.4}(\text{SO}_4)_{1.8} + 20.4\text{H}^+ \leftrightarrow 8\text{Fe}^{3+} + 1.8\text{SO}_4^{2-} + 12.4 \text{H}_2\text{O}$	10.5±2.5
Kawano and Tomita (2001)	$\text{Fe}_8\text{O}_8(\text{OH})_{6.9}(\text{SO}_4)_{1.05} + 21.9\text{H}^+ \leftrightarrow 8\text{Fe}^{3+} + 1.05\text{SO}_4^{2-} + 13.9 \text{H}_2\text{O}$	7.06±0.09
Majzlan et al. (2004)	$\text{Fe}_8\text{O}_8(\text{OH})_6(\text{SO}_4) + 22\text{H}^+ \leftrightarrow 8\text{Fe}^{3+} + \text{SO}_4^{2-} + 14 \text{H}_2\text{O}$	9.6±4